ANALYSIS OF ELECTRICAL ENERGY DISSIPATION IN SUBMERGED-ARC FURNACES PRODUCING SILICOMANGANESE

Joalet Dalene Steenkamp – MINTEK, South Africa
Christopher James Hockaday – MINTEK, South Africa
Johan Petrus Gous – Transalloys, South Africa

The Arc Monitor, or "Arcmon", is a device that was developed by Mintek – a South African-based research council – primarily to quantify the amount of arcing in a submerged-arc furnace in which energy is supplied to the process via an electrical system based on alternating current. Arcmon was installed successfully on industrial-scale silicon, ferrosilicon and ferrochrome furnaces.
Towards the end of 2012 and beginning of 2013, Arcmon was evaluated on two 48 MVA silicomanganese furnaces at Transalloys, based in Emalahleni in South Africa. Arcmon was installed for three months on Furnace #7 and for three months on Furnace #5. One third of Furnace #5 was subsequently, systematically excavated, process and refractory materials sampled, and electrode lengths measured and electrode tip conditions photographed.
The Arcmon results indicated that, in silicomanganese production, up to 15% of the electrical energy utilised, is transferred by arcing i.e. more arcing occurs in a SAF producing silicomanganese, in comparison with charge chrome production (up to 5%), but significantly less than in silicon and ferrosilicon production (20 – 60%). From an operational perspective, Arcmon was able to identify the build-up of hard material below electrode #3, and was utilised as an indicator of process stability.

KEYWORDS: ARCMON – SILICOMANGANESE – SAF – ARCING

INTRODUCTION

Production of silicomanganese at Transalloys

Transalloys is currently the largest producer of silicomanganese in Africa, with its operations based in Emalahleni, South Africa. At Transalloys, silicomanganese is produced by carbothermic reduction of oxide raw materials. Transalloys operates, inter alia, two 48 MVA silicomanganese submerged-arc furnaces [1]. At full production, the 48 MVA furnaces typically produce 175 tons of alloy and 140 tons of slag, per day. ASTM Grade B [2] silicomanganese (16 – 18 %Si, 66 – 68 %Mn, by mass) is produced from a blend of coal, ore briquettes, manganese ore sinter, lumpy manganese ore, SiMn-metal fines, and quartzite [3]. Note that slag from high carbon ferromanganese production, as is typical of the duplex process for silicomanganese production [4], is not included in the feed. The power consumption on these furnaces is typically 3.8 – 4.2 MWh/ton alloy produced [3].

Introducing Arcmon

The Arc Monitor, or "Arcmon", is a device that was developed by Mintek, primarily for measuring the amount of arcing in a submerged-arc furnace (SAF). It is also able to quantify the other parameters of the electrical circuit of the furnaces, such as burden resistance and magnetic reactance. Because this concept of measuring arc information is relatively new, it has been necessary to study the behaviour of various types of ferroalloys, with the aid of the Arcmon, to see how the technology can be applied to the benefit of the process operation. To date, Arcmon has been used successfully on silicon, ferrosilicon and ferrochrome furnaces [5], [6].

Basic principles of transfer of electrical energy in SAFs producing manganese ferroalloys

Submerged-arc smelting is the traditional method applied in ferroalloy production [7], in which electricity supplies the energy required by the endothermic reduction of ore by carbonaceous reductants. The *submerged* part of the name is derived from the fact that the electrodes tips are submerged in a porous charge mix. Whether arcing occurs or not is a function of the commodity produced, and even within a

INDEX

specific commodity, debatable.

General: Matyas et al [7] stated that in submerged-arc smelting, the major portion of the electrical energy is liberated by micro-arcing to an incandescent coke bed floating on the molten bath, and that the technology is applied in the production of ferroalloys, pig iron, silicon metal, and elemental phosphorus. Westley [8] differentiated between ferrosilicon, where a crater is formed between the charge zone and the reaction zone, and slag processes i.e. ferromanganese, silicomanganese, ferrochromium, silico-chromium, and pig iron, where the charge zone is separated from the reaction zone by a coke bed. Both instances introduce modes of transfer of electrical energy other than micro-arcing: Arcing, and resistive heating.

Ferrochrome: When modelling the electrical currents in a SAF producing charge chrome, McDougal [9] found that very little current passes through the charge, whilst current passes into the slag in a relatively small region below the electrode (i.e. resistive heating). This was consistent with the findings of furnace dig-outs [10], in which isolated coke bed zones were observed below the electrodes. Barker et al [6], applying Arcmon technology, determined that very little (less than 5%) arcing occurred in a SAF producing charge chrome, and only after tapping.

Silicon, Ferrosilicon: Sævarsdottir et al [11] stated that in SAF producing silicon, or ferrosilicon, the arcs burn in gas filled cavities or "craters", where the main atomic components of the plasma mixture are silicon, oxygen and carbon. Sævarsdottir and Bakken [12] found, through a combination of modelling and measurements, that 50% of the electrical energy is transferred by arcing. Applying ARCMON technology, Barker et al [5], [6] determined that in both silicon and ferrosilicon smelters, between 20% and 60% of the electrical energy used, is transferred by arcing. They concluded that it was not surprising that both types of furnace behaved similarly from the perspective of arcing and related electrical behaviour, as the processes were very similar: in both processes craters form around electrode tips, and a slag layer is usually absent [6].

High carbon ferromanganese: Lee and Tangstad [13] stated that in the production of high carbon ferromanganese, the required energy for chemical reactions in submerged arc furnaces is provided by resistive heating, with electric current flowing through molten slag and coke bed zones, which is also supported by findings from furnace excavations [4], [14].

Silico-manganese: For silico-manganese production, two schools of thought exist: (a) that the required energy for the chemical reactions is provided by resistive heating, similar to high carbon ferromanganese production [15], and (b) that both arcing and resistive heating occurs as is the case for ferrosilicon production [16].

More light is shed on the silico-manganese process as the paper reports on the measurements obtained by Arcmon on Furnace 5 and Furnace 7 at Transalloys. The paper also provides a comparison between the Arcmon results obtained from Furnace 5, and results obtained from Furnace 7. Lastly the paper provides a comparison between the Arcmon results and the physical findings of the digout of Furnace 5.

BACKGROUND

Basic principles of Arcmon

The equivalent circuit of the furnace, as used for the Arcmon, is shown in Fig. 1. In brief, it consists of a star circuit, with each individual electrode in the furnace corresponding to one of the branches of the star. Each branch then consists of a magnetic inductor, an arc, and a basic burden resistor, all in series. Fig. 1 indicates how the conduction through the burden can be split into an arcing component and a purely resistive component, in series. The equivalent circuit shown here excludes the delta elements that model the pulses in the transformer magnetisation currents. The Arcmon can also accommodate an auxiliary electrode (stinger electrode), typically used to open the tap-hole in Si-metal furnaces, but it was not applicable to this trial.

To distinguish between arcing and resistive conduction, an electrical model of an arc is needed. In the Arcmon, a linearised form of Cassie's model has been used as it provides a reasonably good fit to the observed waveforms [5]. The burden resistors are modelled by using Ohm's law.

INDEX

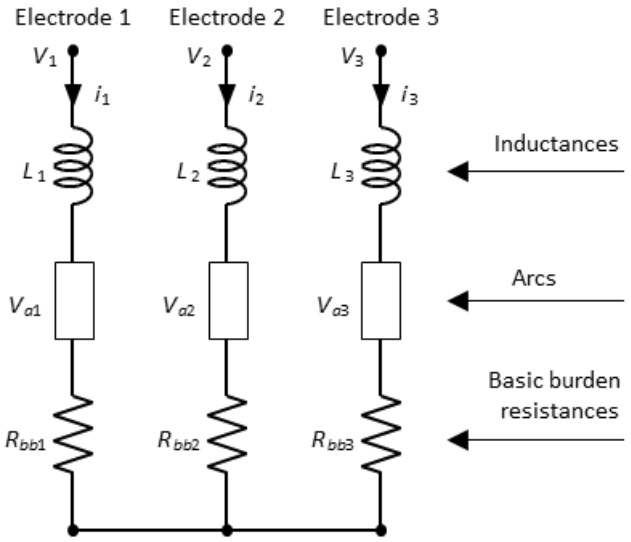

Fig.1 – Equivalent circuit of the furnace

Quantification of arcing and resistive conduction

The primary measurement obtained from Arcmon is the arc voltage, denoted V_a. This is the voltage drop across the arc, as opposed to across the entire electrode to bath ($V_{1,2,3}$), which is conventionally measured. The Arcmon unit is also able to calculate the amount of power dissipated in each of the arcs and each of the resistors R_{bbi} (representing the burden) of the equivalent circuit of a furnace. Through this it is able to calculate the fraction of the total power to the furnace that is dissipated in the arcs, termed the "arc power fraction" ", as defined by the equation below:

$$APF = \frac{P_a}{P_a + P_{bb}} \quad (1)$$

Where, APF is the arc power fraction (dimensionless number), P_a the power dissipated in the arc (measured in kW), and P_{bb} the power dissipated through resistive heating in the burden (measured in kW).

The arc power fraction is another measure that can be used to compare the amount of arcing between the different processes. The usefulness of the arc power fraction as a measurement, as opposed to the individual V_a or R_{bb} signals, arises from the fact that it is either calculated as a single quantity for each electrode or for the furnace as a whole, and it is independent of the power or current levels in the furnace. The arc power fraction also has a direct metallurgical relevance as to how the energy dissipation is split between the various zones within the burden of the furnace.

The power input from resistance heating is related to the square of the electrode current and the burden resistance of the area of conduction:

$$P_{bb} = I_e^2 \times R_{bb} \quad (2)$$

Where, P_{bb} is the power dissipated in the burden (measured in kW), I_e the current in the electrode (measured in kA), and R_{bb} the resistance of the burden (measured in mΩ).

The resistance is roughly proportional to the length of the conduction path from electrode tip to molten bath.

METHOD

Arcmon installation

From September 2012 to March 2013, an Arcmon unit was installed at Transalloys. Arcmon was installed initially for a three month trial on Furnace 7 (week 41 to week 48 of 2012), and then transferred to Furnace 5 for a three month trial (week 50 of 2012 to week 9 of 2013) when it was shut down for excavation, and reline [3]. The Arcmon unit was installed on Furnace 5, right up to the end of the campaign, since the furnace

INDEX

excavation would provide an ideal opportunity to compare arcing data from Arcmon, with physical findings in the furnace.

Excavation of Furnace 5

Furnace 5 was excavated to sample the burden, and refractory material, in one-third of the furnace between electrodes 1 and 3 – see Fig. 2. The excavation method was reported by Gous et al [3], and a number of publications followed on the investigation into wear of the refractory material of the single level tap-hole [17] – [20].

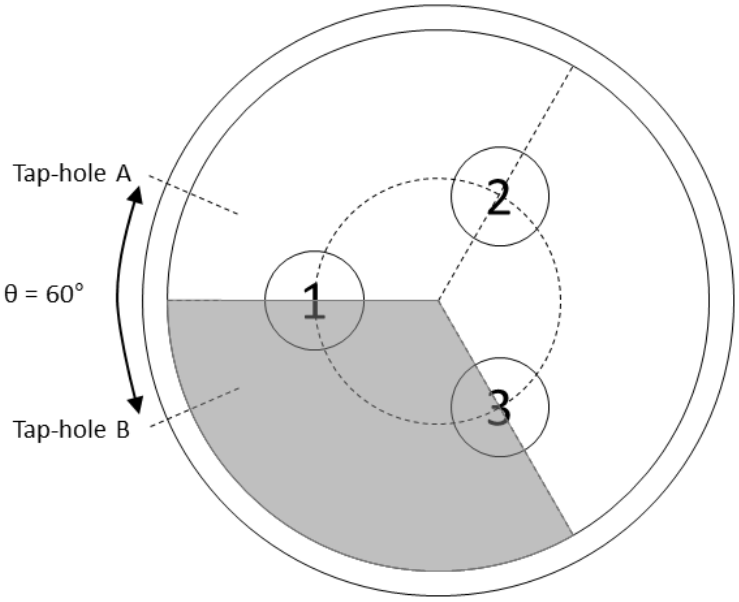

Fig.2 – Schematic of Furnace 5 in plan view where the shaded area indicates the 1/3 of the furnace excavated between electrodes 1 and 3, including tap-hole B

Three weeks prior to switching out Furnace 5, a pressure ring failure on #2 electrode, caused a massive water leak and subsequent downtime of 18.5 hours. Both #1 and #2 electrodes broke one meter below the contact shoes, within 12 hours after the start-up (on February 6th). A two meter stump was removed from #2 electrode, but the broken tip at #1 electrode was pushed into the furnace burden. In the two weeks after the breakages, long slips were taken (± 2m) at #1 and #2 electrodes – excluding normal slipping to compensate for normal burn-off – and corrective action taken to stabilize the process, and to get sufficient penetration of the electrodes.

RESULTS AND DISCUSSION

Excavation of Furnace 5

During furnace excavation, no evidence of the broken electrode was found. The electrode lengths were measured – see Tab. 1 – with the pressure rings on each electrode as reference point, which is dependent on the position of the individual electrode arms and therefore varied between electrodes, or the tap-hole, a constant reference point. Electrode #3 was significantly shorter than the two electrodes that broke-off three weeks earlier.

In silicomanganese production, the presence of a coke bed (≈½ meter high), consisting of slag and carbonaceous reductant, is ideal for stable furnace operations. Knowing the position of the electrode tip is useful for producers of silicomanganese, as it determines where the energy is distributed in the furnace [4],

and could provide an indication of whether a furnace is over-carbon[1], resulting in very large coke beds, or under-carbon[2], resulting in metal that does not meet product specifications, and high electrode wear. At Transalloys, monitoring hearth temperature, measured by thermocouples positioned below each electrode in the hearth, is considered the most suitable way of tracking electrode tip positions – see Fig. 3. As the position of the electrode tip above the tap-hole increases, the distance between the electrode tip and the hearth thermocouple also increases, and therefore a decrease in hearth temperature is expected, assuming all other process conditions being the same. Based on the results in Tab. 1 and Fig. 3, the shortest electrode (#3) had the lowest hearth temperature, but the longest electrode (#2) did not have the highest hearth temperature. As will be seen in Fig. 4 to Fig. 7, the 'coke bed' below electrode #3 consisted of material different from the material below electrode #1 and electrode #2. Differences in heat transfer, and mode of transfer of electrical energy, due to the difference in material, could explain both the position of the tip of electrode #3, and associated hearth temperature, but not the results for electrode #2.

Tab. 1 – Length of each electrode and hearth temperatures

ELECTRODE NUMBER	#1	#2	#3
Electrode length in reference to pressure rings downwards [cm]	345	430	245
Electrode tip above tap-hole [cm]	200	100	250
Average lower hearth temperature over the duration of the ARCMON campaign [°C]	456	405	344

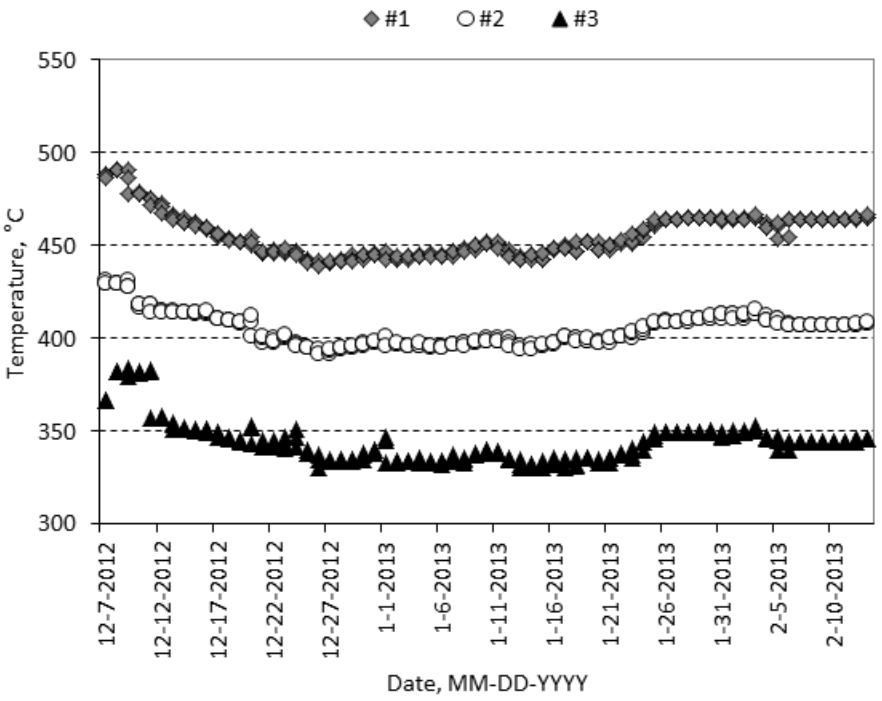

Fig.3 – Lower hearth temperatures (400 mm above bottom steel plate) measured below each electrode

Fig. 4 to Fig. 7 below, reports on observations made, related to electrodes, on Furnace 5 during furnace excavation.

The burden layers below electrode #1 – Fig. 4 (a) – and electrode #2 consisted of a thick coke bed consisting of slag and reductant – Fig. 5 (a) – , followed by a thin metal layer, on top of the hearth refractory

[1] Over-carbon: Furnace condition where carbon builds up, resulting in large coke beds (in the excess of 2 meters), due to the fact that more carbonaceous reductant is charged to the furnace, than what is consumed by the process.
[2] Under-carbon [8]: Furnace condition where the process consumed all the carbonaceous reductant charged to the furnace, and a coke bed is absent.

INDEX

(carbon rammable). A hard[3] build-up was identified below electrode #3 – Fig. 4 (b) and Fig. 5 (b) –, which gave off a 'carbide smell'[4] when sprayed with water. The tips of all three electrodes were submerged in coke bed, even the tip of electrode #3, although the coke bed around the tip of electrode #3 was very small, forming only on top of the hard build-up (see Fig. 7).

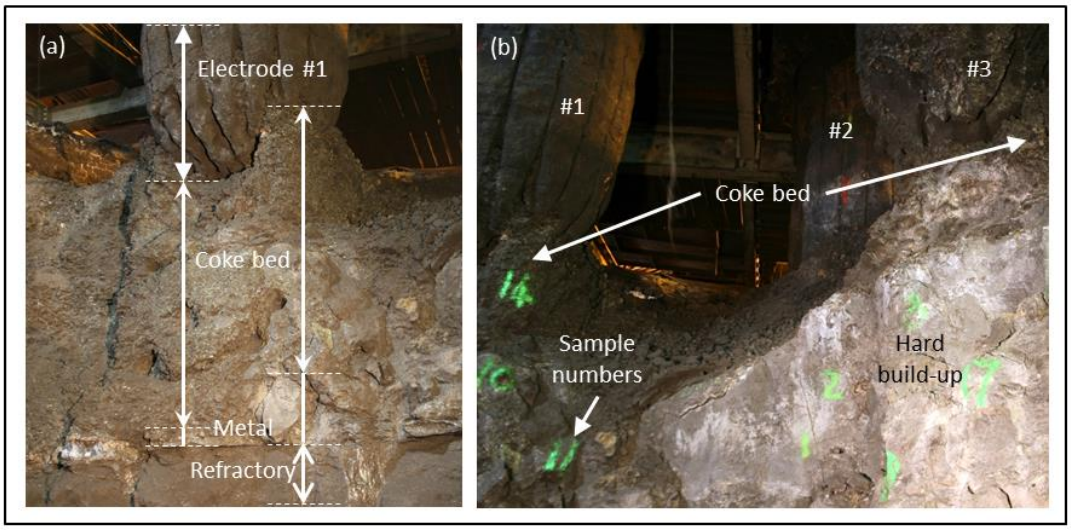

Fig.4 – (a) Different layers below electrode #1: Coke bed zone, metal layer, and hearth refractory layer. Similar layers were also observed below electrode #2, but not below electrode #3. (b) Electrode #3 only had a small coke bed, on top of a hard build-up, that formed between the coke bed and the metal layer. Note: The entire loose burden around the electrodes, was removed by the time the photograph was taken

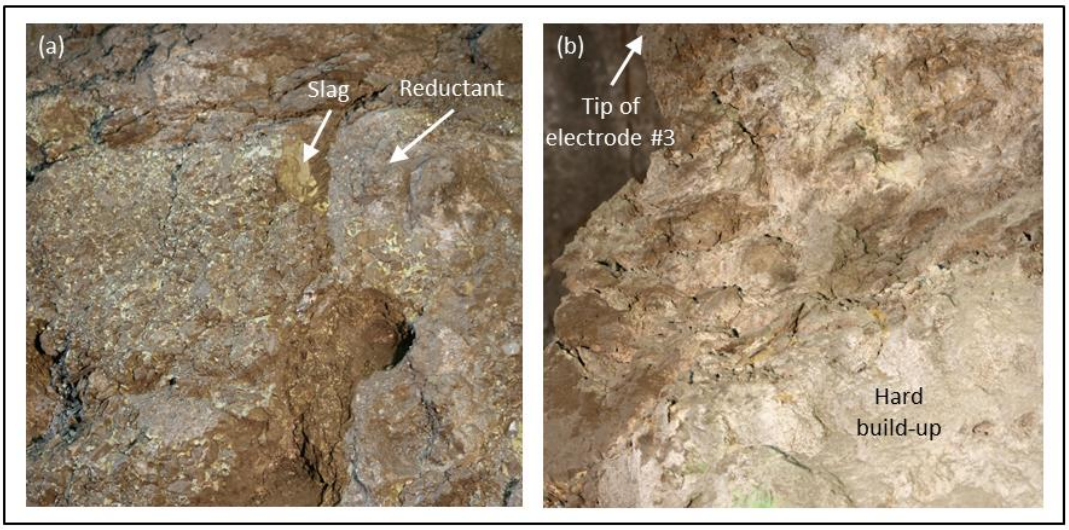

Fig.5 – (a) Higher resolution photograph of coke bed below electrode #1, consisting of slag (green) and reductant (dark—grey). (b) Higher resolution photograph of hard build-up below electrode #3

When removing the coke bed covering the electrode tips, small cavities were observed between the electrode tips, and the coke bed, as illustrated by the photographs of electrode #1, in Fig. 6 and Fig. 7.

Also note the wear pattern on the 1.6 m diameter electrodes, illustrated by the photographs in Fig. 6: The vertical grooves formed during the baking process, and were caused by the steel fins of the steel shell that contains the electrode paste. At the tip, the electrodes wore to a ballpoint pen shape, with the vertical grooves becoming areas of high wear. The upper part of the electrodes, did not show significant wear. The wear pattern observed is similar to the wear pattern observed by Lee and Tangstad [13] on the electrode of a

[3] A qualitative observation: The material below electrode #3 was hard relative to the softer material found below electrodes #1 and #2.
[4] The odour, reminiscent of garlic, typical of the odor emitted by calcium carbide in the presence of water.

INDEX

150 KVA pilot scale furnace that produced HCFeMn.

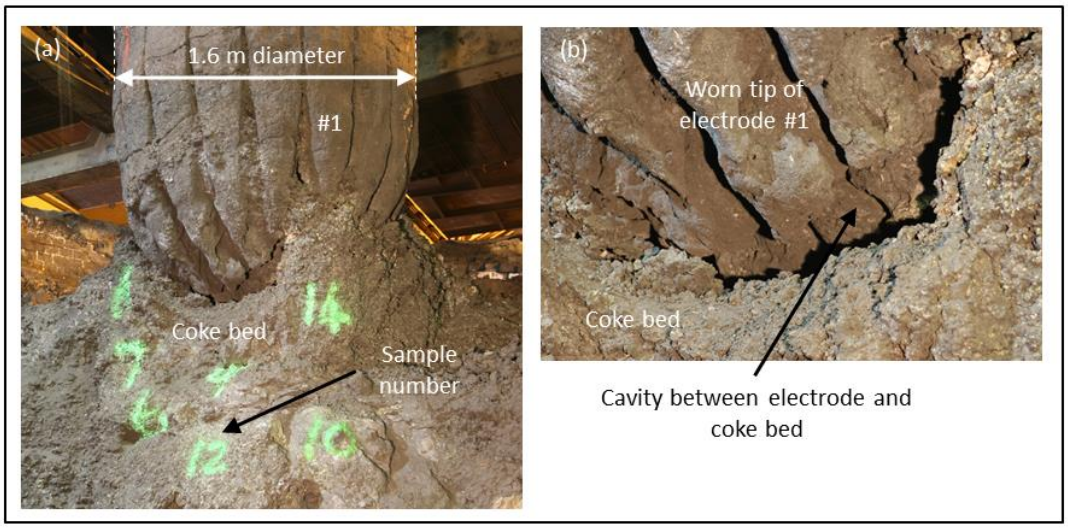

Fig.6 – (a) Electrode #1 with (b) close-up of interface electrode and coke bed, indicating the position of a small cavity between the two. Numbers, spray-painted in green onto the burden, indicate sampling positions and numbers

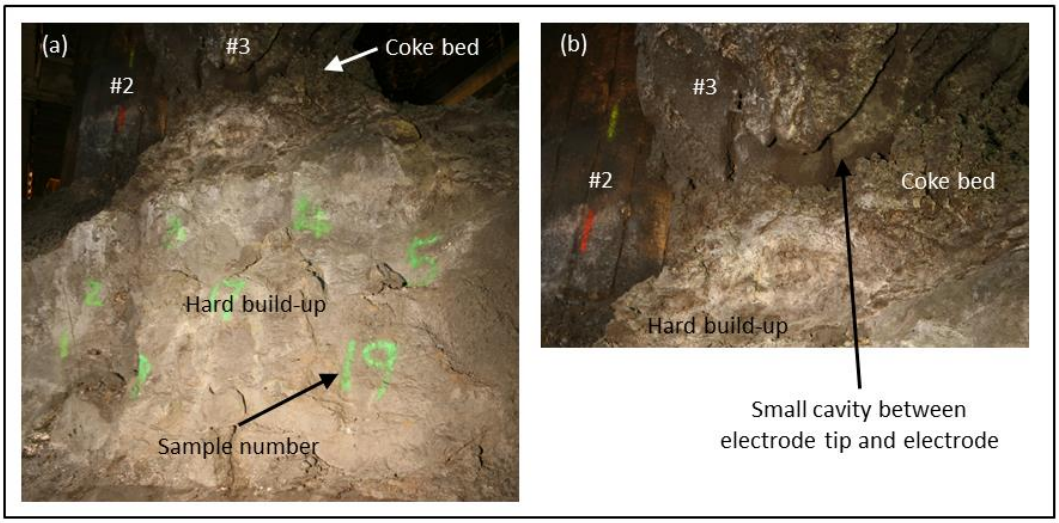

Fig.7 – (a) Electrode #3 with electrode #2 to the back thereof, with (b) close-up of interface electrode and coke bed, indicating the position of a small cavity between the two. Numbers, spray-painted in green onto the burden, indicate sampling positions and numbers

Lee and Tangstad [13] concluded that the observed wear pattern indicated that virtually no electric current flowed across the top furnace charge, in the upper part of furnace, but that it flowed through the molten slag zone and, most intensively, through the coke bed zone. Apart from the cavities that formed below the electrode tips, the same conclusion was made for the electrodes in the Furnace 5.

Quantification of arcing and resistive conduction

Analysis of the Arcmon data recorded for Furnace 5 and Furnace 7, summarised in Tab. 2 and Tab. 3, shows the arc voltage to typically be of the order of 5 V. This is fairly low, considering the electrode-bath voltage at normal operating levels is approximately 150 V. In other words, most of the supply voltage is dropped across (and hence power generated through) the coke bed in the furnace, as opposed to arcing through plasma, as indicated by the low arc power fraction calculated for each electrode. This is in agreement with the observations made during the subsequent excavation of Furnace 5, as described in the previous section.

Indicated in Fig. 8 is the magnitude of the arc voltage in Furnace 5 on December 15th, towards the beginning

INDEX

of the campaign. This specific 24 hour period was selected, as indicative of typical operations i.e. prior to the formation of the hard build-up below electrode #3.

Tab. 2 – Furnace 5 arcing statistics with calculations based on total set of data (consisting of 76 daily average datapoints)

F5	Arc Voltage (V)			Arc Power Fraction (%)		
	Va1	Va2	Va3	APF1	APF2	APF3
Mean	2.13	2.70	5.19	1.4	2.3	4.7
Std Dev	2.06	2.20	2.49	0.8	1.6	2.2

Tab. 3 – Furnace 7 arcing statistics with calculations based on total set of data (consisting of 55 daily average datapoints)

F7	Arc Voltage (V)			Arc Power Fraction (%)		
	Va1	Va2	Va3	APF1	APF2	APF3
Mean	3.99	3.31	3.67	2.7	2.3	2.2
Std Dev	3.44	3.60	3.67	1.2	2.3	1.1

On average, the arc power fraction varied between 0% and 15% (Fig. 8 a). The behaviour of the three electrodes, varied significantly: Arcing at electrode #1, which was the electrode closest to the two single level tap-holes, occurred at significantly lower frequencies, and significantly lower intensities as indicated by arc power fractions less than 25% (Fig. 8 b). Periods of arcing on electrode #1 could also be linked to tapping intervals – the tap-to-tap time was typically 3 hours – as was found for charge chrome production [6]. Arcing on the other two electrodes, occurred at higher frequencies (Fig. 8 c, d), and in the case of electrode #2, higher intensities as indicated by the arc power fractions less than 40% (Fig. 8 c). Higher arc power fractions were also observed during furnace blows and furnace eruptions. No clear correlations between arc power fraction and slag basicity, carbon build-up and holder position could be established.

The differences in arcing behaviour between electrode #1, and electrodes #2 and #3, were partially attributed to the way in which the furnace drained during tapping: The higher the slag – to – coke ratio in a wet coke[5] bed, the less likely arcing is to occur as arcing is not likely to occur in conjunction with slag [6]. During tapping, slag and metal drained simultaneously from the single level tap-hole. As the density of silicomanganese metal is half that of slag – see Appendix A – the metal collects in the bottom of the furnace, above the hearth during production (Fig. 4). Therefore, when the tap-hole is opened, metal drains initially from the furnace. As the tap continues, the slag drains from the furnace. For slag to drain from the furnace, it has to drain from the coke bed. As electrode #1 is located closest to the two tap-holes, and the tap-holes were positioned symmetrically to the electrode (Fig. 2), the coke bed below electrode #1 is most likely to contain slag at all times. During furnace excavation, evidence of a wet coke bed was recorded below electrode #1 (Fig. 4 a, and Fig. 5 a).

[5] In a wet coke bed, the carbonaceous reductant is present in slag. In a dry coke bed, very little slag, if any, is present.

INDEX

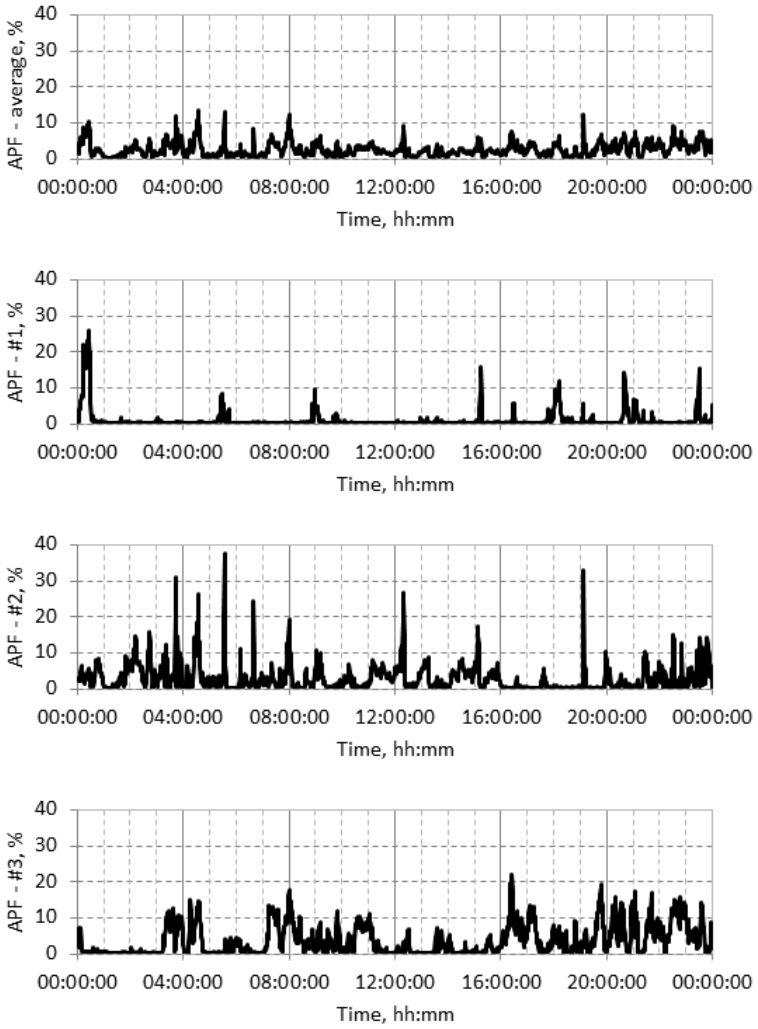

Fig.8 – (a) Magnitude of the arc power fraction in Furnace 5: typical graph over 24 hours. APF – average was the calculated average of the APF's for the three electrodes, APF - #1 for electrode #1, APF - #2 for electrode #2, and APF - #3 for electrode #3

Effect of hard build-up, electrode breakages

The presence of the hard build-up below electrode #3 was detected by Arcmon as indicated by the daily average arc power fraction calculations, presented in Fig. 9, specifically for the time period prior to the water leak into the furnace and subsequent electrode breaks. Where the daily average arc power fractions on electrode #1 and #2 were 2% or less, the daily average arc power fraction on electrode #3 ranged between 4% and 8%. Furthermore, abnormally elevated levels of arcing has been found to be indicative of a short electrode not fully immersed in the wet coke bed [6]. During the excavation of Furnace 5 it was found that Electrode 3 was indeed significantly shorter than the other two electrodes, as summarised in Tab. 1.

Barker et al [6] found that in charge chrome production, the information from Arcmon unequivocally identified the sudden loss of an electrode tip in a large ferro-chrome furnace with restricted electrode movement results, as electrode tip breaks also lead to significantly higher levels of arcing for extended periods (often up to 1 to 2 days), until the electrode can be slipped sufficiently for the tip to return to its original position in the furnace. Although the electrode breaks on electrode #1 and electrode #2 on February 6th, offered the opportunity to study this observation on a silicomanganese furnace, the Arcmon system did not operate between January 30th, and February 8th. From the results in Fig. 9, the daily averaged arc power fractions for electrode #3, once the Arcmon system was back online, returned to its previous pattern. Results on both

INDEX

electrode #1 and electrode #2 indicated that the furnace did not achieve the same level of stability, prior to being switched out for the reline.

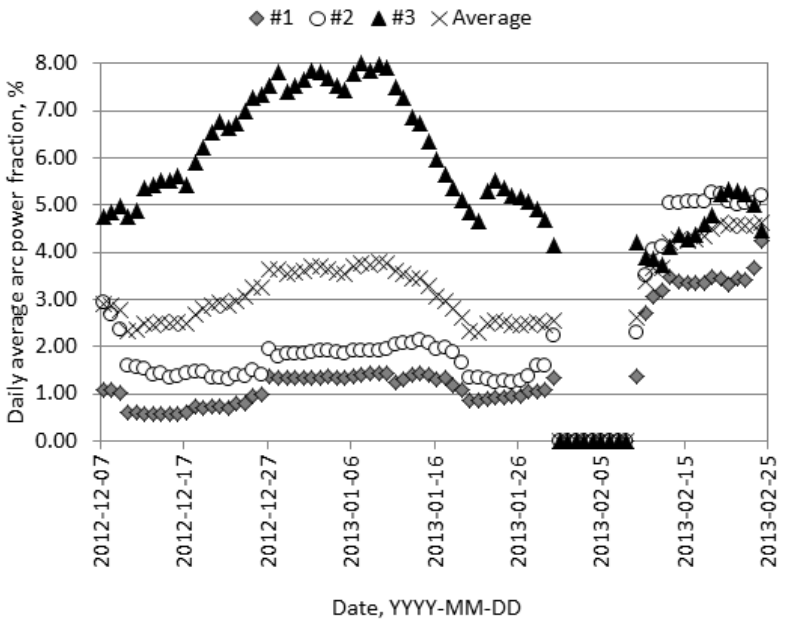

Fig.9 – Calculated daily average arc power fractions over the duration of installation on Furnace 5. APF Average was the calculated average of the daily average APF's for the three electrodes, APF1 for electrode #1, APF2 for electrode #2, and APF for electrode #3

CONCLUSIONS

The Arcmon results indicated that, in silicomanganese production, up to 15% of the electrical energy utilised, is transferred by arcing i.e. more arcing occurs in a SAF producing silicomanganese, in comparison with charge chrome production (up to 5%), but significantly less than in silicon and ferrosilicon production (20 – 60%). Generating similar datasets for other commodities applying SAF technology, i.e. high carbon ferromanganese, will be useful.

From an operational perspective, Arcmon was able to identify the build-up of hard material below electrode #3, and was utilised as an indicator of process stability. Characterisation of the build-up below electrode #3, and comparing the characterization thereof against that of the coke bed samples below electrode #1, will be useful.

Further development of the Arcmon technology, when utilised in conjunction with other instrumentation available on the furnace, as a potential indicator of electrode tip position, will also be useful.

ACKNOWLEDGEMENTS

This paper is published with the permission of Transalloys, and MINTEK after being reviewed internally by Markus Erwee and Herman Lagendijk.

APPENDIX A

Tab. 4 – Density, in tons per meter cube, of industrial SiMn metal and slag

Method		Slag	Metal
Archimedes, in water	Average	2.943	6.314

INDEX

Method		Slag	Metal
10 samples	Stdev	0.002	0.018
Helium picnometry 3 samples	Average	3.128	6.453
	Stdev	0.019	0.225

REFERENCES

[1] J. D. Steenkamp and J. Basson, “The manganese ferroalloys industry in southern Africa,” *J. South. African Inst. Min. Metall.*, vol. 113, pp. 667–676, 2013.

[2] ASTM Standards A483 / A483M - 10, “Standard Specification for Silicomanganese.” ASTM International, West Conshohocken, PA, 2003, pp. 1–2, 2010.

[3] J. P. Gous, J. H. Zietsman, J. D. Steenkamp, and J. J. Sutherland, “Excavation of a 48 MVA silicomanganese submerged-arc SiMn furnace in South Africa – Part I: Methodology and Observations,” in *5th International Symposium on High-Temperature Metallurgical Processing*, 2014, pp. 255–269.

[4] S. E. Olsen, M. Tangstad, and T. Lindstad, *Production of manganese ferroalloys*. Trondheim, Norway: Tapir Academic Press, 2007.

[5] I. J. Barker, M. S. Rennie, C. J. Hockaday, and J. P. Brereton-Stiles, “Modes of electrical conduction in industrial silicon-type furnaces,” in *Silicon for the Chemical Industry VIII*, 2006, pp. 79–90.

[6] I. J. Barker, M. S. Rennie, C. J. Hockaday, and P. J. Brereton-Stiles, “Measurement and control of arcing in a submerged-arc furnace,” in *Infacon XI: Innovation in Ferroalloy Industry*, 2007.

[7] A. G. Matyas, R. C. Francki, K. M. Donaldson, and B. Wasmund, “Application of new technology in the design of high-power electric smelting furnaces,” *CIM Bull.*, vol. 86, no. 972, pp. 92–99, 1993.

[8] J. Westly, “Resistance and heat distribution in a submerged-arc furnace,” in *INFACON I*, 1974, pp. 121–127.

[9] I. Mc Dougall, “Finite element modelling of electric currents in AC submerged arc furnaces,” in *Infacon XI: Innovation in Ferroalloy Industry*, 2007, pp. 630–637.

[10] E. Ringdalen and J. Eilertsen, “Excavation of a 54 MVA HC-ferrochromium furnace,” in *Ninth International Ferroalloy Congress and the Manganese 2001 Health Issues Symposium*, 2001, pp. 166–173.

[11] G. Sævarsdottir, M. T. Jonsson, and J. A. Bakken, “Arc-electrode interactions in silicon and ferrosilicon furnaces,” in *INFACON X: Transformation through technology*, 2004, pp. 593–604.

[12] G. Sævarsdottir and J. A. Bakken, “Current distribution in submerged arc furnaces for silicon metal / ferrosilicon production,” in *Infacon XII: Sustainable future*, 2010, pp. 717–728.

[13] Y. E. Lee and M. Tangstad, “Electric parameters for an efficient smelting performance of HCFeMn alloy,” in *The Twelfth International Ferroalloys Congress*, 2010, pp. 569–578.

[14] N. A. Barcza, A. Koursaris, J. B. See, and W. A. Gericke, “The ‘dig out’ of a 75 MVA high-carbon ferromanganese electric smelting furnace,” in *Electric Furnace Conference Proceedings*, 1979, pp. 19–33.

[15] M. Tangstad, “Personal communication.” 2015.

[16] J.Basson, “Personal communication.” 2015.

[17] J. D. Steenkamp, “Chemical wear of carbon-based refractory materials in a silicomanganese furnace tap-hole,” University of Pretoria, 2014.

[18] J. D. Steenkamp, J. P. Gous, P. C. Pistorius, M. Tangstad, and J. H. Zietsman, “Wear analysis of a taphole from a SiMn production furnace J.,” in *Furnace Tapping Conference 2014*, 2014, pp. 51–64.

[19] J. D. Steenkamp, P. C. Pistorius, and M. Tangstad, “Chemical wear analysis of a tap-hole on a SiMn production furnace,” *J. South. African Inst. Min. Metall.*, vol. 115, no. 3, pp. 199–208, 2015.

[20] J. D. Steenkamp and P. C. Pistorius, “Chemical wear of carbon-based refractory materials in a silicomanganese furnace tap-hole,” in *INFACON XIV*, 2015, pp. 505–510.

INDEX